

Effect of NiAl content on phases and microstructures of TiC–TiB₂–NiAl composites fabricated by reaction synthesis

Hong-zhi CUI, Li MA, Li-li CAO, Fang-lei TENG, Ning CUI

School of Materials Science and Engineering, Shandong University of Science and Technology, Qingdao 266590, China

Received 28 January 2013; accepted 6 June 2013

Abstract: TiC–TiB₂–NiAl composites were fabricated by self-propagating high temperature reaction synthesis (SHS) with Ti, B₄C, Ni and Al powders as raw materials. The effects of NiAl content on phase constituents and microstructures were investigated. The results show that the reaction products are composed of TiB₂, TiC and NiAl. The content of NiAl increases with the adding of Ni+Al in green compacts. TiB₂, TiC and NiAl grains present in different shapes in the matrix, TiB₂ being in hexagonal or rectangular shapes, TiC in spherical shapes, and NiAl squeezed into the gaps of TiC and TiB₂ grains. With the increase of NiAl content, the grains of TiC–TiB₂–NiAl composites are refined, their density and compressive strength are improved, and the shapes of TiC grains become spherical instead of irregular ones. Finally, the fracture mechanism of the composites transforms from intergranular fracture mode to the compounded fracture mode of intergranular fracture and transgranular fracture.

Key words: TiC–TiB₂–NiAl; self-propagating high temperature reaction synthesis (SHS); composites; microstructure

1 Introduction

TiC–TiB₂ composites possess a series of advantages such as high hardness and melting point, preferable electrical conductivity, high wear and corrosion resistance, fine impact resistance and high temperature stability [1]. Hence, they are very promising high-temperature structural ceramic materials which can be applied as heat components [2], cutting tool material and mold [3,4], protective armor, cathodes for Hall–Heroult cells [1] and gas thermal spraying material [5].

So far, many methods about preparing TiC–TiB₂ composites such as reaction sintering (RS) [6], spark plasma sintering (SPS) [7,8], high-energy ball milling [9], directional solidification [2] and combustion synthesis [10,11], have been reported. Among them, self-propagating high-temperature synthesis technology (SHS) (i.e. combustion synthesis) has been regarded as the most convenient one because of its high efficiency, energy conservation, high quality products, and simply experimental equipment.

However, the higher brittleness of the TiC–TiB₂

composites limits their application. In addition, because of the high melting point, high covalent bond coordination and the low self-diffusion coefficient of TiC–TiB₂, it is difficult to obtain the dense materials [12,13]. In order to improve their density and toughness, many researchers proposed to add metal, ceramic or intermetallics into TiC–TiB₂ [14–17]. By adding Ni/Mo into TiC–TiB₂, the TiC and TiB₂ particles showed equiaxed and prismatic morphologies respectively and distributed uniformly, and also the hardness and fracture toughness of the composites were improved significantly [14]. ZHU et al [17] prepared TiC–TiB₂/Cu composites. The morphology and the size of TiC and TiB₂ particles changed with the addition of Cu. With the increase of Cu content, TiB₂ changed from long strips to short rods and the aspect ratio decreased gradually. The morphology of TiC grains became regular and closed to torispherical or spherical in shapes. The sizes of TiC and TiB₂ particles decreased from 5–8 μm to 1–3 μm.

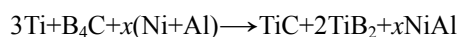
NiAl compounds that belonging to long range order intermetallics possess the advantages of high melting point, low density, good oxidation resistance and heat conduction performance, and can be widely used as high temperature structure material and coating material

[18,19]. Many reports involved the fabrication of NiAl intermetallics and their composites, such as porous NiAl intermetallics with pressureless sintering reaction [20,21], NiAl–TiC–Al₂O₃ composites by vacuum sintering [22] and high energy ball milling [23]. In particular, many researchers focused on SHS method by which NiAl [24], NiAl–Al₂O₃ [25], TiC–NiAl [26], (TiB₂–Al₂O₃)/NiAl [27] and ZrB₂/TiB₂–NiAl [28] have been obtained.

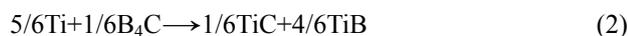
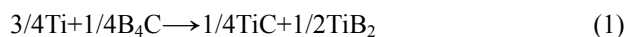
Based on the above analysis, adding NiAl intermetallics into TiC–TiB₂ to synthesize TiC–TiB₂–NiAl composites could be a prospective way to improve the properties. Up to now, few reports about TiC–TiB₂–NiAl composites and their microstructures have been published. In the present work, TiC–TiB₂–NiAl composites are prepared by SHS with Ti, B₄C, Ni and Al as raw materials, and the effects of NiAl content are analyzed on phase constitutions, microstructure morphologies, compressive strength and fracture mode of the products.

2 Thermodynamic calculation of TiC–TiB₂–NiAl

In this experiment, Ti, B₄C, Ni and Al powders were used as raw powders to produce TiC–TiB₂–NiAl composites by SHS, and the phase composition in the products could be changed by varying the mole ratio of the reactants. But the mole ratios of Ti to B₄C and Ni to Al are fixed to 3:1 and 1:1 respectively. During the synthesis process, the possible comprehensive reaction in the mixture may act as the following expression:



where x represents the mole ratio of NiAl ($x=0, 1, 2$ and 3). The possible sole reactions are as follows:



According to the thermodynamics data and calculation formula [29], the standard mole enthalpies and Gibbs free energy of a Ti–B₄C–Ni–Al system calculated in this study are shown in Fig. 1. Figure 1(a) indicates that reactions (1)–(8) are thermodynamically feasible ($\Delta G < 0$), and Fig. 1(b) indicates that all reactions are exothermic ($\Delta H < 0$). In comparison of reactions from (1) to (8) comprehensively, reactions (1), (2) and (3)

have the thermo-dynamical priority. Compared reaction (1) with (2) which maybe occur in Ti–B₄C, the thermodynamic feasibility of reaction (1) is much larger than reaction (2). Thus, the Ti–B₄C–Ni–Al system may react along the paths of reactions (1) and (3), and their final products would be composed of TiC, TiB₂ and NiAl as expected.

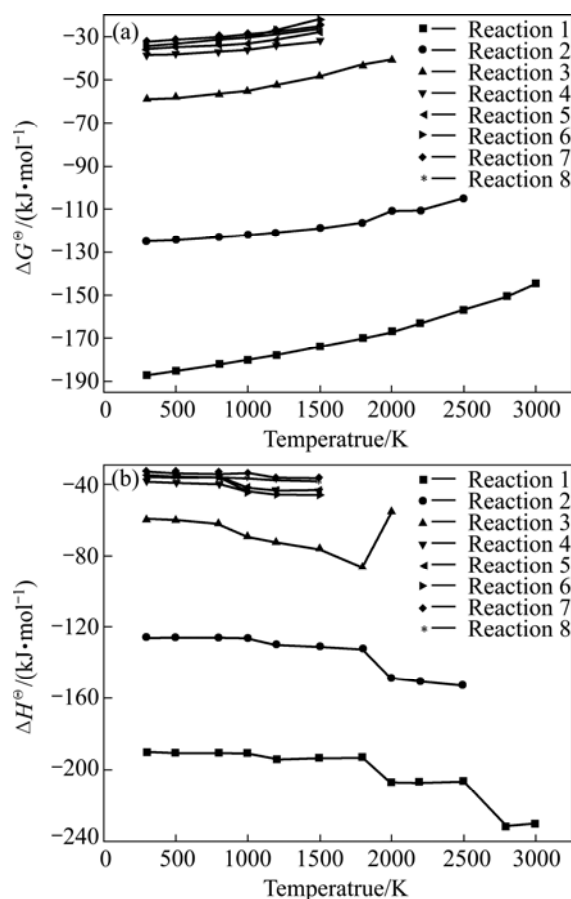


Fig. 1 Change of standard Gibbs free energy (a) and standard molar enthalpy (b) in possible reactions of Ti–B₄C–Ni–Al system at different temperatures

Table 1 shows the calculated T_{ad} in different groups. The T_{ad} values of all the groups are higher than 1800 K, indicating that all the mentioned reactions could spontaneously maintain once ignited [30], namely, the SHS in the mixture could occur.

Table 1 T_{ad} of Ti–B₄C–Ni–Al system with different contents of Ni–Al

Group	3Ti+ B ₄ C	3Ti+B ₄ C+ 1(Ni+Al)	3Ti+B ₄ C+ 2(Ni+Al)	3Ti+B ₄ C+ 3(Ni+Al)
T_{ad}/K	3193	3193	2972	2769

3 Experimental

The raw powders of Ti, B₄C and Ni, Al and their specifications are shown in Table 2. After being weighed,

the powders were mixed for 1 h in a three-dimensional mixing machine to ensure their homogeneity. Then the mixtures were put into a home-made mold to shape the samples into cylinders of about $d20\text{ mm}\times 20\text{ mm}$ at a pressure of 170 MPa. The compacts were preheated at 300 °C for about 30 min in a drying oven, and then taken out, ignited with a live tungsten wire ring to initiate the SHS reaction.

Table 2 Specification and origin of raw powders

Powder	Purity/%	Size/ μm	Origin
Ti	99	38–50	Enterprise group chemical reagent Co., Ltd
B ₄ C	99	7–10	Forward boron carbide eases Co., Ltd
Ni	99.5	38	Enterprise group chemical reagent Co., Ltd
Al	99.5	50–75	Enterprise group chemical reagent Co., Ltd

The compressive strengths of the samples were measured by an electronic universal testing machine (Model WDW3100) and their relative densities were tested by the Archimedes drainage method. Part of the pieces were ground into powders to undergo phase constitution analysis by an X-ray diffraction instrument (XRD, model D/Max 2500PC Rigaku, Japan). The morphologies of the fracture and microstructure were observed by scanning electron microscopy (SEM, Model KYKY2800B). The polished surface of the specimen was subjected to electron probe microanalysis (EPMA, model JXA–8230) to analyze the microstructure and element distribution.

4 Results

4.1 Phase analysis

Figure 2 shows the XRD results of the products. The reaction products consist of only TiC and TiB₂ phases in the Ti–B₄C system with no Ni+Al, without Ti, B₄C or intermediate phases such as TiB. When adding Ni+Al into Ti–B₄C system, NiAl phases emerge besides the TiC and TiB₂ phases, while other compounds such as Ni₃Al, TiAl and NiTi phases do not exist in the productions. With the increase of Ni+Al content, the relative intensity of the NiAl diffraction peaks increase apparently, but the phase components keep the same as TiC, TiB₂ and NiAl, which corresponds with the thermodynamic calculation.

4.2 Microstructure analysis

Figure 3 shows the microstructure of the products. A number of pores exist in TiC–TiB₂ composites and the relative density is about 60% (see Fig. 3(a)). After the

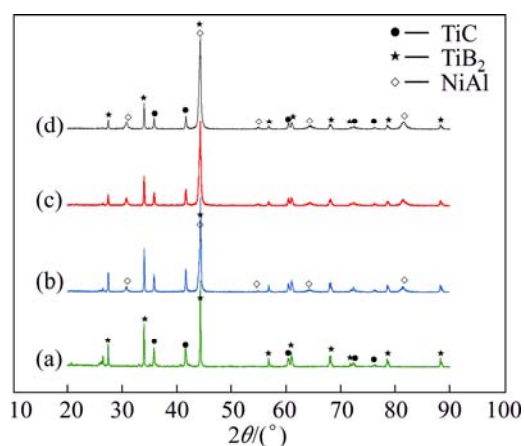


Fig. 2 XRD patterns of products with different contents of Ni+Al in 3Ti+B₄C system: (a) 3Ti+B₄C; (b) 3Ti+B₄C+1(Ni+Al); (c) 3Ti+B₄C+2(Ni+Al); (d) 3Ti+B₄C+3(Ni+Al)

addition of NiAl, the number of the pores decreases and the density is improved significantly (see Figs. 3(b)–(d)).

Figure 3(a) shows that TiC–TiB₂ composites are constituted by two different phases: one in dark grey color and in hexagonal or rectangular shapes with the size of 3–5 μm , and the other one in light grey color and in irregular shapes which distributed in the gaps of the dark grey particles. Figures. 3(b)–(d) show that the microstructure of TiC–TiB₂–NiAl composites consists of three phases. Besides the dark grey and light grey phases in Fig. 3(a), another bright white phase appears, and it exhibits good wettability with the former two. The grains of the three phases are closely packed together. The dark grey phases present the same hexagonal or rectangular shapes in Fig. 3(a), but the light grey phases change to spherical particles instead of irregular ones. The bright white phases seem to have a higher plasticity compared with the other two phases and their grains fill in the gaps between the dark and light grey grains perfectly. With the increase of NiAl content, the sizes of both dark and light grey grains become small, in other words, the grains are refined. In Fig. 3(d), the sizes of dark and light particles decrease to 1–2 μm .

EPMA images and elements distribution of TiC–TiB₂ composites are shown in Fig. 4. Figure 4(a) shows the microstructure of TiC–TiB₂ composites at high magnification. It shows the regular dark grey and irregular light grey grains clearly. Figure 4(b) shows that element B is mainly distributed in dark grey areas with hexagonal or rectangular shapes. Figure 4(c) reveals that element C is mainly distributed in light grey areas with irregular shapes. Element Ti exists in both the dark and light grey areas but contains a greater proportion in the light grey areas. According to the XRD results, the reaction products of Ti–B₄C are only TiC and TiB₂. Consequently, it can be deduced that the dark grey

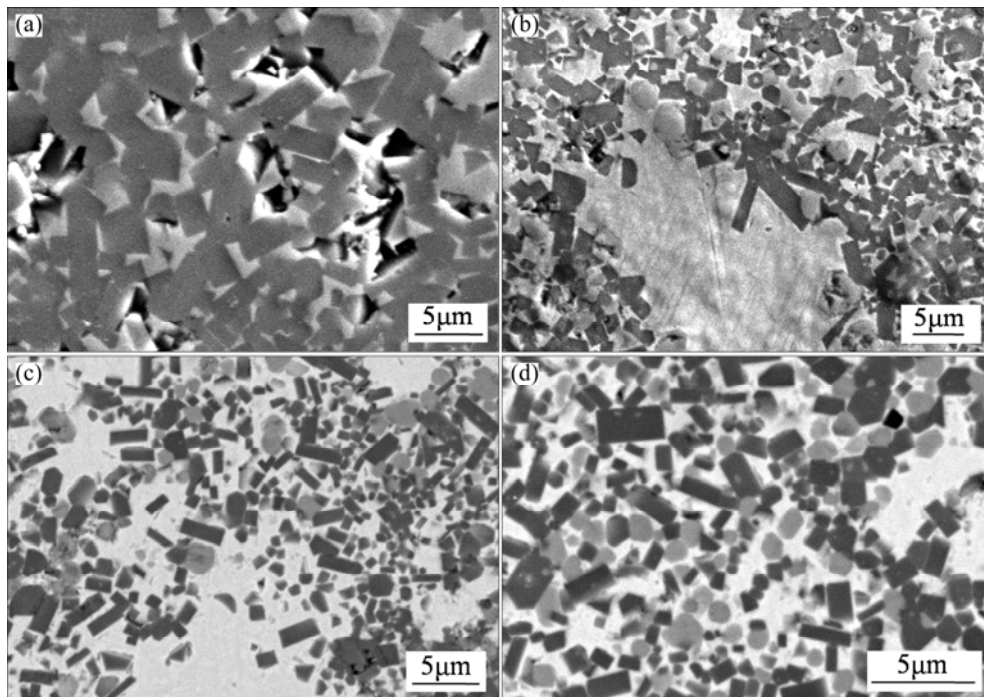


Fig. 3 SEM images of TiC-TiB₂ and TiC-TiB₂-NiAl composites: (a) TiC-2TiB₂; (b) TiC-2TiB₂-1NiAl; (c) TiC-2TiB₂-2NiAl; (d) TiC-2TiB₂-3NiAl

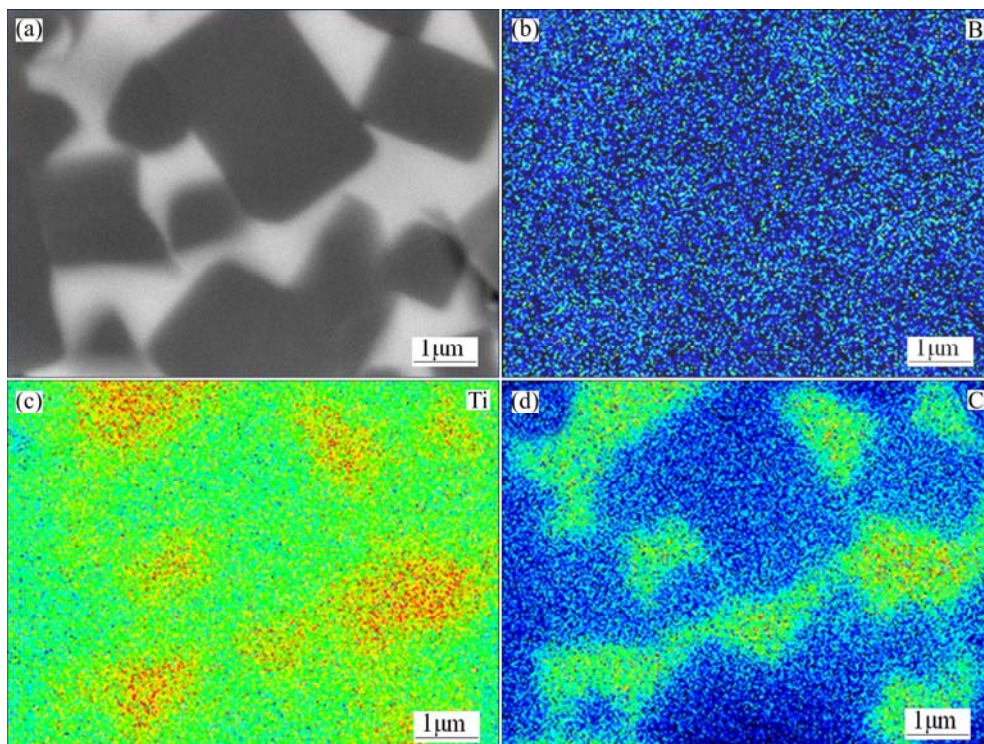


Fig. 4 EPMA image (a) and elements distribution (b, c, d) of TiC-TiB₂ composites (color and brightness represent intensity of corresponding element)

particles in hexagonal or rectangular shapes are TiB₂, and the light grey phases with irregular shapes filling in the gaps of TiB₂ grains are TiC. Figure 5 shows the microstructure and the elements distribution of TiC-TiB₂-NiAl composites. Figure 5(a) shows the

microstructure of TiC-2TiB₂-1NiAl at high magnification. The hexagonal or rectangular dark grey grains, spherical light grey grains and bright white grains which represent three different phases can be seen clearly. Figures 5(b) and (c) show that the distribution of elements

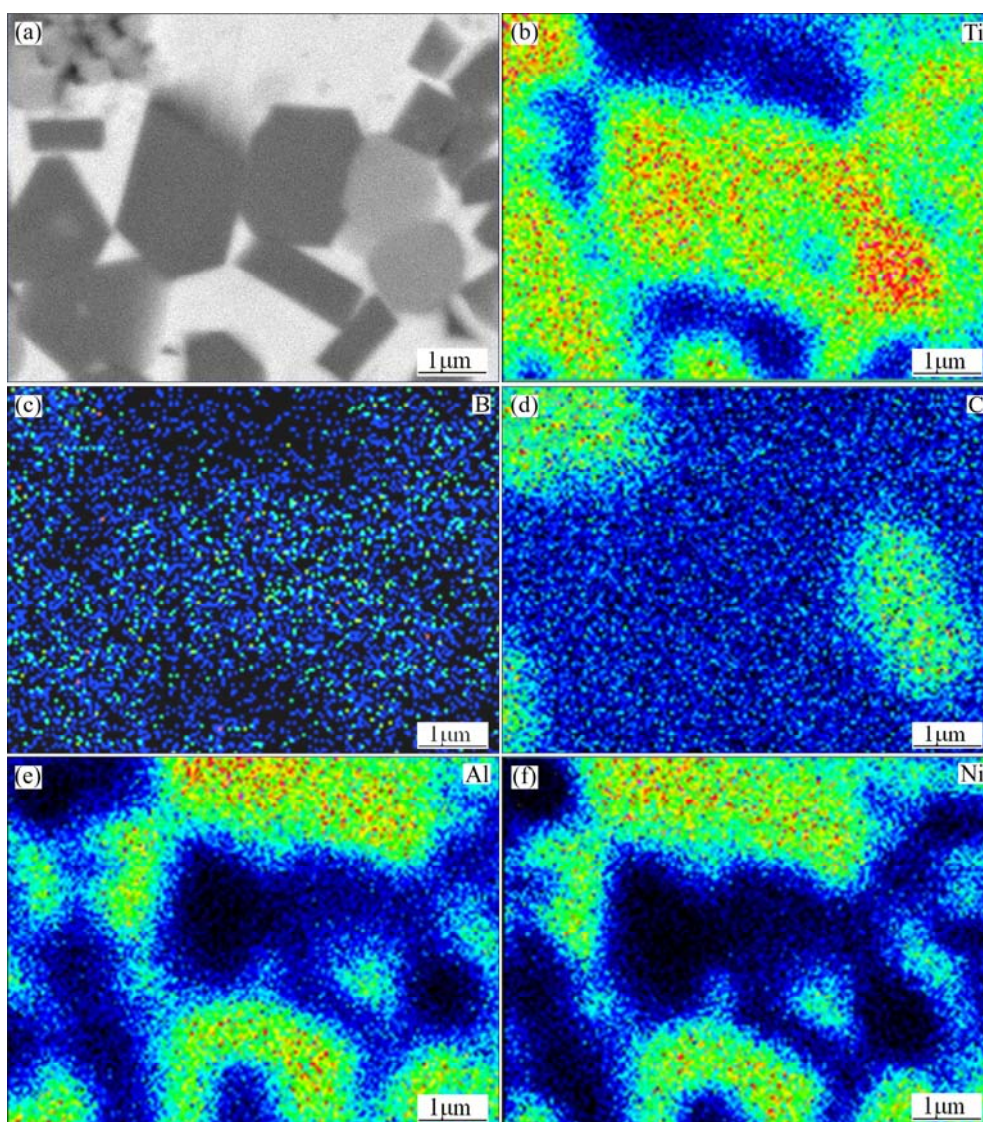


Fig. 5 EPMA image (a) and elements distribution (b, c, d, e, f) of TiC–TiB₂–NiAl (color and brightness represent the intensity of corresponding element)

B, C and Ti keeps the same contour as Fig. 4. Elements Ni and Al are mainly distributed in the bright white areas with irregular shapes. Combined with XRD results, the dark grey and light grey phases are TiB₂ and TiC respectively, and the bright white phases with irregular shapes in the gaps of TiC and TiB₂ are NiAl. Furthermore, after the adding of NiAl, the shapes of the light grey phases alternate from the amorphous to the spherical, which have not been reported in previous publications.

4.3 Compressive strength and fracture analysis

The results of the compressive strength of TiC–TiB₂–NiAl composites are shown in Table 3. Since the process of the SHS reaction was free of pressure, there are a number of pores in TiC–TiB₂ composites, and the maximum porosity reaches 40% approximately, according to Table 4. It can be safely concluded that the

addition of Ni+Al, i.e the formation of NiAl, improves the compressive strength and density of TiC–TiB₂ composites. And with the increase of NiAl content, the compressive strength and density of TiC–TiB₂–NiAl composites are increased gradually.

Table 3 Compressive strength of TiC–TiB₂–NiAl composites

Group	TiC– 2TiB ₂	TiC– 2TiB ₂ –1NiAl	TiC– 2TiB ₂ –2NiAl	TiC– 2TiB ₂ –3NiAl
Strength/ MPa	33.32	44.28	48.32	51.06

Table 4 Relative density of TiC–TiB₂–NiAl composites

Group	TiC– 2TiB ₂	TiC– 2TiB ₂ –1NiAl	TiC– 2TiB ₂ –2NiAl	TiC– 2TiB ₂ –3NiAl
Relative density/%	59.96	62.96	66.93	69.96

The fracture morphologies of the composites are shown in Fig. 6. TiC–TiB₂ composites mainly perform intergranular fracture occurring at the boundary of TiB₂ and TiC (see Fig. 6(a)). The surface is rather flat without any plastic deformation, and the fracture reveals the original morphology of grains. Some regular pits which may be formed by the extracting of TiB₂ particles could be observed clearly. However, after the adding of Ni+Al, the products of TiC–TiB₂–NiAl composites perform both intergranular and transgranular fractures. The intergranular fracture still takes place at the boundary of TiB₂ and TiC, while the transgranular fracture mainly happens in NiAl grains. Notable cleavage patterns with part of lacerate traces are observed on NiAl grains (see Fig. 6(d)). The marked characteristics mean a pronounced change of fracture mechanism from the intergranular one to the transgranular one with the forming NiAl in TiC–TiB₂ composites. The above tendency is more evidently with the increase of NiAl in TiC–TiB₂–NiAl composites.

5 Discussion

During the SHS process, a huge amount of heat was released instantly, and the gas existing in the interspace of raw powders or adsorbed on their surfaces expanded and escaped from the products simultaneously. This may result in the formation of pores and even small cracks in the production, especially in the case of pressureless.

The calculated T_{ad} of Ti–B₄C system is 3193 K and it is as high as the melting point of TiC which is the highest one among TiC, TiB₂ and NiAl. So after reaction, TiC grains would nucleate and grow up prior to TiB₂ due to their higher melting point and the faster diffusion rate of C element. TiB₂ has the C32 type structure of hexagonal system and small plane growth style. The base surface (0001) prefers to grow along [0001] direction. In this way TiB₂ particles tend to form hexagonal and rectangular shapes [31]. TiC shows perfect plasticity at high temperature [1], and would be squeezed into the gaps of TiB₂ grains and in irregular shapes with the growing of TiB₂ grains. If adding Ni+Al into Ti–B₄C, the T_{ad} of reaction decreases. But, it is still much higher than the melting points of Ni, Al and NiAl. During the reaction of Ti+B₄C+Ni+Al, Ni and Al which have lower melting point could melt and surround Ti and B₄C particles. This would provide liquid channels for the diffusion of elements, especially for B and C that come from the decomposition of B₄C. As a result, the reaction rate in Ti+B₄C+Ni+Al mixture and the formation rate of TiC, TiB₂ are accelerated. During the reaction, and at the temperature between the melting point of TiB₂ (3193 K) and NiAl (1912 K) [29], TiB₂ grains begin to nuclear and grow. Owing to the high thermal conductivity of NiAl, the cooling rate in TiC–TiB₂–NiAl composites is accelerated and the subcooling degree is also enlarged. This can improve the nucleation rate of TiC and TiB₂, and be beneficial to get fine TiC and TiB₂ particles.

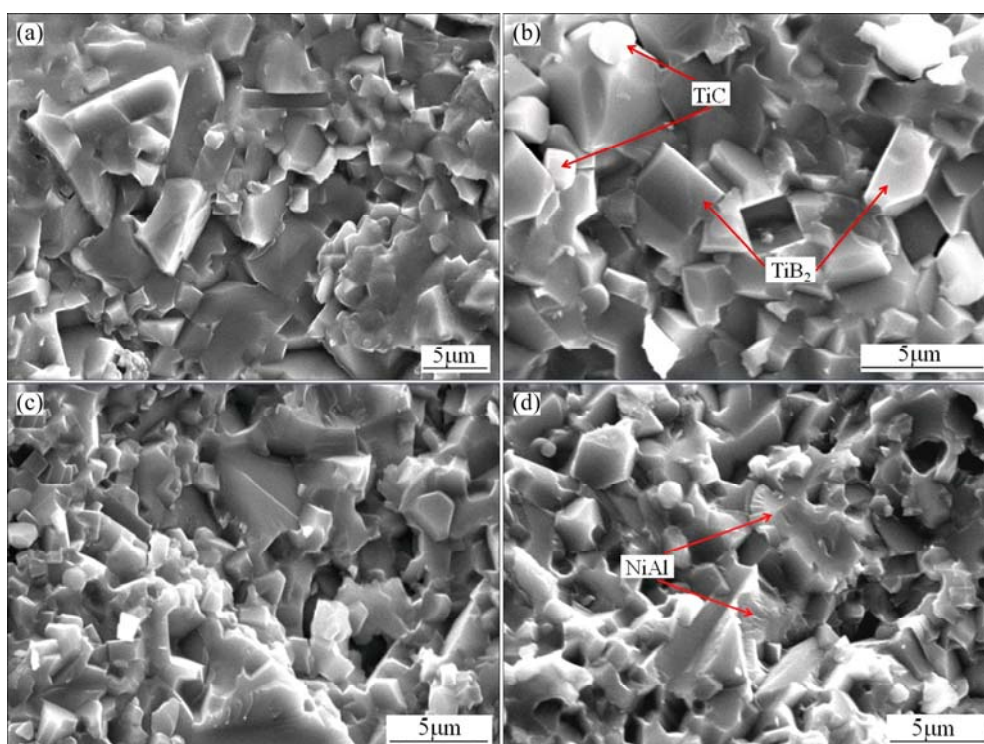


Fig. 6 SEM images showing fracture surface of TiC–TiB₂ and TiC–TiB₂–NiAl composites: (a) TiC–2TiB₂; (b) TiC–2TiB₂–1NiAl; (c) TiC–2TiB₂–2NiAl; (d) TiC–2TiB₂–3NiAl

Furthermore, the existence of NiAl liquid would provide the more free or less stiff space for the growth of TiB₂ grains. The boundary of TiB₂ grains can extend into the liquid NiAl instead of squeezing into the plastic TiC. In this way, the spherical TiC grains could maintain their shapes of the spherical integrality. As time goes by, NiAl would solidify and fill in the intervals of TiB₂ and TiC grains, forming the denser composites. Besides, NiAl phases with the better ductility [32] also consume more crack propagating energy during the fracture of TiC–TiB₂–NiAl composites compared with pure TiC–TiB₂. The refined TiC and TiB₂ particles, higher density, better ductility of NiAl accompanied by the adding of Ni+Al, make contributions to improve the compressive strength of the TiC–TiB₂–NiAl composites. And this was not mentioned in previous article about the fabrication and microstructure of TC–TiB₂.

6 Conclusions

1) TiC–TiB₂–NiAl composites were prepared by SHS with Ti, B₄C, Ni, Al powders as raw materials. TiB₂ showed hexagonal or rectangular shapes; TiC grains changed to spherical shapes from the irregular shapes which distributed in the gaps of TiB₂ grains in TiC–TiB₂ composites; NiAl showed irregular shapes filling in the gaps between TiC and TiB₂ grains.

2) By adding Ni+Al and forming NiAl phases with high thermal conductivity, the cooling rate was accelerated and the subcooling degree was enlarged in the reacting system. This refined the size of both TiC and TiB₂ particles and increased the density and compressive strength in TiC–TiB₂–NiAl composites.

3) The fracture of TiC–TiB₂–NiAl composites followed a mixed fracture of intergranular and transgranular modes. Intergranular fracture occurred at the boundary of TiC and TiB₂ grains, while transgranular fracture was found mainly in the NiAl grains.

References

- [1] VALLAURI D, ATIAS ADRIAN I C, CHRYSANTHOU A. TiC–TiB₂ composites: A review of phase relationships, processing and properties [J]. *Journal of the European Ceramic Society*, 2008, 28(8): 1697–1713.
- [2] LI W J, TU R, GOTO T. Preparation of directionally solidified TiB₂–TiC eutectic composites by a floating zone method [J]. *Materials Letters*, 2006, 60(6): 839–843.
- [3] ZOU B, HUANG C Z, SONG J P, LIU Z Y, LIU L, ZHAO Y. Effects of sintering processes on mechanical properties and microstructure of TiB₂–TiC+8wt% nano–Ni composite ceramic cutting tool material [J]. *Materials Science and Engineering A*, 2012, 540: 235–244.
- [4] YAN Jian-hui, ZHANG Hou-an, LI Yi-min. Mechanical properties and oxidation resistance behavior of TiC–TiB₂ reinforced MoSi₂ composites [J]. *The Chinese Journal of Nonferrous Metals*, 2009, 19(8): 1424–1430. (in Chinese)
- [5] WANG Z T, ZHOU X H, ZHAO G G. Microstructure and formation mechanism of in-situ TiC–TiB₂/Fe composite coating [J]. *Transactions of Nonferrous Metals Society of China*, 2008, 18(4): 831–835.
- [6] AKHTAR F, HASAN F. Reactive sintering and properties of TiB₂ and TiC porous cermets [J]. *Materials Letters*, 2008, 62(8–9): 1242–1245.
- [7] LI B H, LIU Y, LI J, CAO H, HE L. Effect of sintering process on the microstructures and properties of in situ TiB₂–TiC reinforced steel matrix composites produced by spark plasma sintering [J]. *Journal of Materials Processing Technology*, 2010, 210(1): 91–95.
- [8] CAO Guo-jian, XU Hong-yu, ZHENG Zhen-zhu, GENG Lin, Naka MASAOKI. Grain size effect on cyclic oxidation of (TiB₂+TiC)/Ni₃Al composites [J]. *Transactions of Nonferrous Metals Society of China*, 2012, 22: 1588–1593.
- [9] LI J L, LI F, HU K A, ZHOU Y. TiB₂/TiC nanocomposite powder fabricated via high energy ball milling [J]. *Journal of the European Ceramic Society*, 2001, 21(16): 2829–2833.
- [10] SHEN P, ZOU B L, JIN S B, JIANG Q C. Reaction mechanism in self-propagating high temperature synthesis of TiC–TiB₂/Al composites from an Al–Ti–B₄C system[J]. *Materials Science and Engineering A*, 2007, 454–455: 300–309.
- [11] XU Q, ZHANG X H, HAN J C, HE X D, KVANIN V L. Combustion synthesis and densification of titanium diboride-copper matrix composite [J]. *Materials Letters*, 2003, 57(28): 4439–4444.
- [12] VALLAURI D, DEORSOLA F A. Synthesis of TiC–TiB₂–Ni cermets by thermal explosion under pressure [J]. *Materials Research Bulletin*, 2009, 44(7): 1528–1533.
- [13] LU J B, SHU S L, QIU F, WANG Y W, JIANG Q C. Compression properties and abrasive wear behavior of high volume fraction TiC_x–TiB₂/Cu composites fabricated by combustion synthesis and hot press consolidation [J]. *Materials & Design*, 2012, 40: 157–162.
- [14] ZOU B, HUANG C Z, SONG J P, LIU Z Y, LIU L, ZHAO Y. Mechanical properties and microstructure of TiB₂–TiC composite ceramic cutting tool material [J]. *International Journal of Refractory Metals and Hard Materials*, 2012, 35: 1–9.
- [15] ZOU B L, SHEN P, JIANG Q C. Dependence of the SHS reaction behavior and product on B₄C particle size in Al–Ti–B₄C and Al–TiO₂–B₄C systems [J]. *Materials Research Bulletin*, 2009, 44(3): 499–504.
- [16] MASANTA M, SHARIFF S M, ROY CHOUDHURY A. Tribological behavior of TiB₂–TiC–Al₂O₃ composite coating synthesized by combined SHS and laser technology [J]. *Surface and Coatings Technology*, 2010, 204(16–17): 2527–2538.
- [17] ZHU Chun-cheng, ZHANG Xing-hong, HE Xiao-dong. Self-propagating high-temperature synthesis of TiC–TiB₂/Cu ceramic-matrix composite [J]. *Journal of Inorganic Materials*, 2003, 18(4): 872–878. (in Chinese)
- [18] GUO Jian-ting. Research progress of intermetallic NiAl alloys [J]. *Journal of Central South University: Science and Technology*, 2007, 38(6): 1013–1027. (in Chinese)
- [19] OU Tao-ping, CAO Guang-hui. Preparation processes of Ni–Al-based coatings and their oxidation resistance [J]. *The Chinese Journal of Nonferrous Metals*, 2012, 22(6): 1725–1730. (in Chinese)
- [20] DONG H X, JIANG Y, HE Y H, SONG M, ZOU J, XU N P, HUANG B Y, LIU C T, LIAW P K. Formation of porous Ni–Al intermetallics through pressureless reaction synthesis [J]. *Journal of Alloys and Compounds*, 2009, 484(1–2): 907–913.
- [21] DONG Hong-xing, LIU Qiu-ping, HE Yue-hui, WU Liang. Pore formation mechanism of porous NiAl intermetallics [J]. *The Chinese Journal of Nonferrous Metals*, 2013, 23(2): 474–479. (in Chinese)
- [22] WANG Zhen-sheng, ZHOU Lan-zhang, GUO Jian-ting, HU Zhuang-qi. Wear behavior of in situ composite NiAl–Al₂O₃–TiC at high temperature [J]. *Tribology*, 2008, 28(6): 497–502. (in Chinese)

- [23] DERCZ G, PAJAK L, FORMANEK B. Dispersion analysis of NiAl–TiC–Al₂O₃ composite powder ground in a high-energy attritor mill [J]. *Journal of Materials Processing Technology*, 2006, 175(1–3): 334–337.
- [24] CURFS C, TURRILLAS X, VAUGHAN G B M, TERRY A E, KVICK Å, RODRÍGUEZ M A. Al–Ni intermetallics obtained by SHS: A time-resolved X-ray diffraction study [J]. *Intermetallics*, 2007, 15(9): 1163–1171.
- [25] ZHU X, ZHANG T, MORRIS V, MARCHANT D. Combustion synthesis of NiAl/Al₂O₃ composites by induction heating [J]. *Intermetallics*, 2010, 18(6): 1197–1204.
- [26] CURFS C, CANO I G, VAUGHAN G B M, TURRILLAS X, KVICK Å, RODRÍGUEZ M A. TiC–NiAl composites obtained by SHS: A time-resolved XRD study [J]. *Journal of the European Ceramic Society*, 2002, 22(7): 1039–1044.
- [27] CAO Li-li, CUI Hong-zhi, WU Jie, TANG Hua-jie. Microstructures of (TiB₂–Al₂O₃)/NiAl composite prepared by in-situ reaction synthesis [J]. *The Chinese Journal of Nonferrous Metals*, 2012, 22(10): 2790–2796. (in Chinese)
- [28] ERDEM ÇAMURLU H, MAGLIA F. Self-propagating high-temperature synthesis of ZrB₂ or TiB₂ reinforced Ni–Al composite powder [J]. *Journal of Alloys and Compounds*, 2009, 478(1–2): 721–725.
- [29] YE Da-lun, HU Jian-hua. *Practical inorganic thermodynamic data manual* [M]. Beijing: Metallurgical Industry Press, 2002. (in Chinese)
- [30] YIN Sheng. *Combustion synthesis* [M]. Beijing: Metallurgical Industry Press, 1999. (in Chinese)
- [31] LE Yong-kang, ZHANG Jian-ping, CHEN Dong, MA Nai-heng, WANG Hao-wei, MAO Jian-wei. Growth behavior of in-situ synthesized TiB₂ particle [J]. *Special Casting & Nonferrous Alloys*, 2008, 28(2): 102–105. (in Chinese)
- [32] GUO Jian-ting. *Ordered intermetallic compound NiAl alloy* [M]. Beijing: Science Publications, 2003. (in Chinese)

NiAl 含量对反应合成 TiC–TiB₂–NiAl 物相及组织结构的影响

崔洪芝, 马丽, 曹丽丽, 滕方磊, 崔宁

山东科技大学 材料科学与工程学院, 青岛 266590

摘要: 以 Ti、B₄C、Ni、Al 粉末为原料, 通过自蔓延高温反应合成工艺(SHS)制备 TiC–TiB₂–NiAl 复合材料, 研究 NiAl 含量对反应产物的物相组成及组织结构的影响。结果表明: Ti+B₄C+Ni+Al 粉末 SHS 反应产物的物相组成为 TiB₂、TiC 和 NiAl, 随着 Ni+Al 添加量的增多, NiAl 相的衍射峰强度逐渐增强; TiB₂、TiC 和 NiAl 在基体中呈现不同的形态, 其中 TiB₂ 呈六边形或长条状, TiC 呈圆形, NiAl 填充在 TiC 和 TiB₂ 颗粒之间; 随着 NiAl 含量的增加, TiC–TiB₂–NiAl 复合材料的晶粒逐渐被细化, 致密度和抗压强度均被提高, TiC 的形态由不规则形状转变为圆形。复合材料的断裂方式由单纯的沿晶断裂转变为混合的沿晶断裂和穿晶断裂。

关键词: TiC–TiB₂–NiAl; 自蔓延高温反应合成工艺(SHS); 复合材料; 组织结构

(Edited by Hua YANG)